JOURNAL OF VIROLOGY, Apr. 2005, p. 5035–5046 Vol. 79, No. 8
0022-538X/05/$08.00+0 doi:10.1128/JVI.79.8.5935–5046.2005

Two Gamma Interferon-Activated Site-Like Elements in the Human Cytomegalovirus Major Immediate-Early Promoter/Enhancer Are Important for Viral Replication†

James Netterwald,[1] Shaojun Yang,[1] Weijia Wang,[1] Salena Ghanny,[2] Michael Cody,[2] Patricia Soteropoulos,[1,2] Bin Tian,[3] Walter Dunn,[4] Fenyong Liu,[4] and Hua Zhu[1]*

Department of Microbiology and Molecular Genetics[1] and Department of Molecular Biology and Biochemistry,[3] New Jersey Medical School, University of Medicine and Dentistry of New Jersey, and Center for Applied Genomics, Public Health Research Institute, International Center for Public Health,[2] Newark, New Jersey, and Division of Infectious Diseases, School of Public Health, University of California, Berkeley, California[4]

Received 9 September 2004/Accepted 10 December 2004

Human cytomegalovirus (HCMV) infection directly initiates a signal transduction pathway that leads to activation of a large number of cellular interferon-stimulated genes (ISGs). Our previous studies demonstrated that two interferon response elements, the interferon-stimulated response element and gamma interferon-activated site (GAS), in the ISG promoters serve as HCMV response sites (VRS). Interestingly, two GAS-like VRS elements (VRS1) were also present in the HCMV major immediate-early promoter-enhancer (MIEP/E). In this study, the importance of these VRS elements in viral replication was investigated. We demonstrate that the expression of the major IE genes, IE1 and IE2, is interferon inducible. To understand the biological significance of this signal transduction pathway in HCMV major IE expression, the two VRS1 in the MIEP/E were mutated. Mutant HCMVs in which the VRS elements were deleted or that contained point mutations grew dramatically more slowly than wild-type virus at a low multiplicity of infection (MOI). Insertion of wild-type VRS1 into the mutant viral genome rescued the slow growth phenotype. Furthermore, the expression levels of major IE RNAs and proteins were greatly reduced during infection with the VRS mutants at a low MOI. HCMV microarray analysis indicated that infection of host cells with the VRS mutant virus resulted in a global reduction in the expression of viral genes. Collectively, these data demonstrate that the two VRS elements in the MIEP/E are necessary for efficient viral gene expression and replication. This study suggests that although the HCMV-initiated signal transduction pathway results in induction of cellular antiviral genes, it also functions to stimulate viral major IE gene expression. This might be a new viral strategy in which the pathway is used to regulate gene expression and play a role in reactivation.

Human cytomegalovirus (HCMV) is a ubiquitous human pathogen that is a major cause of disease and death in immunocompromised individuals, especially in transplant recipients and AIDS patients. It also is a leading viral cause of birth defects (7). HCMV infection triggers a series of cellular responses and modulates normal cellular functions, including initiating signal transduction pathways, alternating cell cycle controls, preventing apoptosis, and allowing escape from the immune system (8, 14, 19, 22, 27, 45).

HCMV has the largest genome in the human herpesvirus family, which is about 236-kb long and may encode as many as 250 open reading frames (ORFs) (12, 35, 36). The viral genes are expressed temporally and are classified into immediate-early (IE), early, and late genes (32). HCMV contains two major IE genes, IE1 and IE2, encoding 72-kDa (491 amino acids [aa]) and 86-kDa (579 aa) proteins, respectively, which are the first viral genes expressed after infection and are crucial for HCMV early and late gene expression as well as viral DNA replication. Mutational analyses of IE2 have shown that IE2 is essential for viral replication (17, 24, 46). In contrast, an IE1 deletion mutant virus grows normally at a high multiplicity of infection (MOI) but shows severe growth defects at a low MOI (15, 16, 34). The mechanism of how a high MOI can overcome IE1 deficiency is not clear.

IE1 and IE2 are transcribed from a very strong HCMV major IE promoter-enhancer (MIEP/E). The enhancer region initially was defined as bp −118 to −524 relative to the +1 transcription start site of major IE RNAs (4). Later, it was expanded to encompass bp −65 to −550 (26). A variety of transcription factor-binding sites are located in the enhancer region, resulting in strong expression of IE1 and IE2 once the viral DNA arrives in the nucleus (33). Mutational analyses indicated that deletion of the distal enhancer region (−300 to −582) caused a substantial growth defect at a low MOI, suggesting that important elements are located in this region (25).

HCMV infection disrupts the cellular Jak-Stat signal transduction pathway (28–30). However, it also initiates a not-yet-identified signal pathway that leads to the activation of a large number of interferon (IFN)-stimulated genes (ISGs) (50, 51). Since UV-inactivated HCMV or noninfectious viral particles are able to induce ISGs, HCMV entry into the host cell is sufficient to induce ISGs (50, 51). Furthermore, this activity does not require protein synthesis and is independent of IFNs and other cytokines (51). The viral components directly re-

* Corresponding author. Mailing address: Department of Microbiology and Molecular Genetics, UMDNJ—New Jersey Medical School, 225 Warren St., Newark, NJ 07101-1709. Phone: (973) 972-6488, ext. 2-6488. Fax: (973) 972-8981. E-mail: zhuhu@umdnj.edu.

† Supplemental material for this article may be found at http://jvi.asm.org/.

sponsible for this induction are not completely clear yet, but the viral envelope glycoproteins, especially gB and gH, and fusion between the viral envelope and cellular membrane are required for this induction (5, 38, 40). Our recent studies showed that two IFN response elements in the ISG promoters, the IFN-stimulated response element (ISRE) and IFN-γ-activated site (GAS), serve as HCMV response sites (VRS), and consensus sequences of these elements are critical for HCMV entry-mediated transcriptional activation (47). Several cellular proteins are activated after HCMV infection and form specific complexes with VRS (47).

The biological significance of this HCMV-initiated signal transduction pathway for the viral replication, per se, is unknown. In this study, the function of the two VRS elements (VRS1) in the distal region of the HCMV MIEP/E, from bp −380 to −510, was investigated. Deletion and point mutations in these VRS elements were shown to reduce virus production at a low MOI. This growth defect is likely due to low-level expression of the viral IE1 and IE2 genes which results in a global reduction of viral gene expression.

MATERIALS AND METHODS

Cells and viruses. Primary human foreskin fibroblast (HFF) cells were cultured in Dulbecco's modified Eagle's medium supplemented with 10% fetal bovine serum, 100 U of penicillin-streptomycin/ml, and 2.5 μg of amphotericin B/ml at 37°C in a humidified incubator with 5% CO_2. HFF cells used in this study were between passages 8 and 20. *Escherichia coli* strain DY380 (43, 48) was used as the host cell for mutagenesis of the viral genome. The HCMV AD169 strain was obtained from the American Type Culture Collection. The HCMV AD169 bacterial artificial chromosome (BAC) strain ($AD169_{BAC}$) was a gift from T. Shenk and is similar to the one described in reference 49, except the Cre gene is not inserted into the HCMV genome. The BAC vector is flanked by two loxP sites. UV-inactivated HCMV was prepared essentially as described elsewhere (51), with modification. Briefly, an appropriate amount of virus (up to 5 ml) was added to a 10-cm dish (without a cover) and exposed to UV light six times at the auto-cross-link setting using the UV Stratalinker 1800 machine (Stratagene, La Jolla, Calif.). The virus solution was mixed after every exposure to ensure even irradiation. Inactivation by this procedure was verified by viral infectivity and IE1/IE2 expression as described in reference 51.

Inhibition of ISG activation. HFF cells were infected with AD169 at an MOI of 3 for 8 h in the presence of dimethyl sulfoxide (DMSO; control) or different kinase inhibitors. The protein tyrosine kinase inhibitor genistein was purchased from Gibco BRL (Rockville, Md.) and dissolved in DMSO to yield a 20-mg/ml stock solution. A second protein tyrosine kinase inhibitor, herbimycin A, was purchased from Sigma (St. Louis, Mo.) and dissolved in DMSO to yield a 3 μM stock solution. The protein kinase C (PKC) inhibitor, H7, and the PKA inhibitor, HA1004, were obtained from Calbiochem (La Jolla, Calif.) and dissolved in DMSO to yield 10 mM stock solutions. The double-stranded RNA (dsRNA)-dependent kinase (PKR) inhibitor, 2-aminopurine (2-AP), and the cytosolic phospholipase A2 (cPLA2) inhibitor, quinacrine, were obtained from Sigma. 2-AP was prepared as a 1 M stock solution in H_2O and boiled to dissolve before use. Quinacrine was dissolved in phosphate-buffered saline to yield a 10 mM stock solution.

Stimulation of HCMV major IE expression by IFNs. HFF cells were infected with AD169 at an MOI of 0.5 for 8 h. Five hundred units of IFN-α/ml or 5 ng of IFN-γ (Sigma)/ml was added to the cells either 2 h before infection or 2 to 4 h after infection. HCMV IE1 RNA and protein levels were measured by Northern blotting and Western blotting as described in reference 51.

Generation of VRS deletion mutant. The method to construct the recombinant HCMVs employed BAC technology with a highly efficient *E. coli* recombination system as described previously (13). To generate a deletion of both VRS sites in HCMV MIEP/E, $AD169_{BAC}$ DNA was electroporated into *E. coli* strain DY380 (48). A Kan^r and lacZ (*kan*/*lacZ*) cassette was PCR amplified from a plasmid, pGEM/T-Pac-1-Kan/LacZ (a gift from T. Shenk). In order to introduce the desired mutation, the *kan*/*lacZ* primers were designed to include a 40-base sequence homologous to the flanking sequence of the VRS element in the MIEP/E (VRSΔF, 5′-GTA ATC AAT TAC GGG GTC ATT AGT TCA TAG CCC ATA TAT GGA GTT CCG CGC AGA TGC ATA AGG AGA AAA T; VRSΔR, 5′-ACG TCA ATA GGG GGC GTA CTT GGC ATA TGA TAC ACT TGA TGT ACT GCC AAG AGT CAG TGA GCG AGG AAG C). Approximately 200 ng of this *kan*/*lacZ* cassette was electroporated into DY380 carrying $AD169_{BAC}$, and transformants were selected on a Luria-Bertani agar plate containing 12.5 μg of chloramphenicol/ml, 50 μg of kanamycin/ml, 80 μg of 5-bromo-4-chloro-3-indolyl-β-D-galactopyranoside, and 100 mM dioxane-free isopropyl-β-D-thiogalactopyranoside. The blue, kanamycin-resistant colonies were the AD169VRS-Δ mutants. The correct clones were verified by PCR using three sets of primers. The first set amplified only the VRS element: 1F (5′-TCC GCG TTA CAT AA CCT CGA GTA AAT GGC CCG CCT G) and 1R (5′-TGC CAA GTG GGC AGT TAA TCT AGA ATA CTC CAC CCA TTG), giving a ~130-bp product. The second set amplified the left side of the *kan*/*lacZ* cassette insertion: 2F (5′-AGA TCT GGC ATA TTG AAA ATG TCG CCG ATG) and 2R (5′-CCT TGC AGC ACA TCC CCC TTT C), giving a 634-bp product. The third set amplified the right side of the *kan*/*lacZ* cassette insertion: 3F (5′-CAT AAC ACC CCT TGT ATT ACT GTT TAT G) and 3R (5′-GCG GCC GGG CAC TGG GGA CGG TGG TG), producing a 1-kb fragment.

Generation of VRS base-pair substitution mutant and its rescue virus. To facilitate the generation of the VRS point mutant and rescue clones, pGEM-lox-zeo was constructed. A zeocin resistance gene expression cassette (zeo^r), under the control of the *E. coli* EM7 promoter, was amplified by PCR from a plasmid, pCMV/zeo (Invitrogen, Inc., Carlsbad, Calif.), using primers containing loxP sites: zeo-loxP-F (5′-AGA TCT ATA ACT TCG TAT AAT GTA TGC TAT ACG AAG TTA TGG AAC GGA CCG TGT TGA C) and zeo-loxP-R (5′-GGA TCC ATA ACT TCG TAT AAT GTA TGC TAT ACG AAG TTA TCA AGT TTC GAG GTC GAG GTG). This 550-bp PCR product was cloned into a pGEM-T vector (Promega, Madison, Wis.) to produce pGEM-lox-zeo.

To generate point mutations in the VRS elements, they were mutated sequentially by two-step PCR using $AD169_{BAC}$ DNA as a template, resulting in a total of three base-pair exchanges in the GAS consensus sequences. The mutated VRS element was inserted between the SphI and BamHI sites of pGEM-lox-zeo to produce pGEM-lox-VRS-P. The 750-bp fragment containing the VRS mutant sequence and the zeo^r cassette then was amplified by PCR using primers VRS-homo-F (5′-GCA TGC TTA CGG GGT CAT TAG TTC ATA G) and VRS-homo-R (CAT AAT GCC AGG CGG GCC ATT TAC CGT CAT TGA CGT CAA TAG GGG GCG GCC GCA CTA GTG ATG GAT C) and electroporated into DY380 harboring AD169VRS-Δ. The transformants were selected on a Luria-Bertani agar plate containing 12.5 μg of chloramphenicol/ml and 50 μg of zeocin/ml. The resulting colonies, AD169VRS-P, should contain mutated VRS elements inserted into the MIEP/E region by homologous recombination.

To generate a rescue clone of AD169VRS-P, the mutated VRS fragment in the AD169VRS-P genome was deleted by using the *kan*/*lacZ* cassette as described above. Then, the *kan*/*lacZ* cassette was replaced by a wild-type VRS element as described above, resulting in AD169VRS-R.

Generation of the mutant and rescue viruses from the AD169 BAC DNA clones. To generate the VRS mutant and rescue viruses, the BAC DNAs were isolated from DY380 or DH10B and electroporated into HFF cells as described elsewhere (24). A plasmid, pGS403, expressing phage P1 Cre recombinase (49), was cotransfected with the BAC DNAs so that the BAC vector (also flanked by two loxP sites) and zeo^r cassette were removed from the resulting recombinant viruses.

Growth curve and plaque assays. HFF cells in six-well plates were infected at an MOI of 0.1 or 1 for growth curve analysis. At the indicated times, both intracellular and extracellular virus titers were determined. Infected cells and culture medium were collected and centrifuged to separate the supernatant and pellet. Pellets were resuspended in 50 μl of medium, and the cells were lysed by two cycles of rapidly freezing in ethanol cooled with dry ice and thawing in 37°C water. The supernatant and the pellet were then combined, and the cell debris was removed by centrifugation. Virus titers were determined in triplicate by plaque assay on monolayers of HFF cells.

Luciferase assays and EMSA. To measure the transcriptional activity of the mutated VRS elements, the wild-type and mutated VRS elements were created by two-step PCR. In the first step, the VRS elements were amplified from pGEM-lox-zeo-VRS-R and pGEM-lox-zeo-VRS-P, respectively, using CMV-VRS-F (AGA TCT CCC ATA TAT ATG GAG TTC CGC G) and CMV-VRS-R (ACG TCG GCG ACT CGA GTA GTA CAC TTG ATG TAC TGC C). In the second step, a portion of the *isg54k* promoter was amplified from episomal plasmid pElu-NRS (47), using the two primers P4 (CTA CTC GAG TCG CGA CGT AAC GTC AGC TGA AGG GAA ACA) and P2 (ACG TCG ACT CGA GTA GAA ATT GGC AGG ACT CTT T). The two reaction mixtures were diluted 1:100 and mixed with CMV-VRS-F and P2 primers for a second PCR to create a 400-bp PCR product that inserted the HCMV VRS sites into the *isg54k* promoter. The PCR fragments were cloned into the BglII and

HindIII sites of pElu-Basic (47) to generate pElu-VRS-W and pElu-VRS-P reporter plasmids. These two plasmids and the two previously constructed plasmids, pElu-GAS and pElu-GAS^m (47), were transfected into HFF cells. After transfection, the cells were cultured for 10 days to allow ISGs to be quiescent (the transfection procedure activates ISGs), and then luciferase activities were measured as described in reference 47. The protein-binding activity of the mutated VRS element also was measured by electrophoretic mobility shift assays (EMSA) as described in reference 47.

DNA, RNA, and antibody-based analyses. DNA, RNA, and antibody-based analyses were performed as described in references 24 and 51. The monoclonal antibodies used in this study were specific against HCMV pp65 (65–8) (39), IE1 (1B12) (52), IE1/2 (mAB810; Chemicon, Temecula, Calif.), and actin (clone 80; Boehringer, Mannheim, Germany).

HCMV microarray production. Oligonucleotides (65-mers) were designed (Sigma-Genosys, The Woodlands, Tex.) to each of the 194 predicted unique ORFs of HCMV strain AD169 (GenBank accession number NC_001347), with additional gene sequences from the Toledo strain (GenBank accession number U33331) that are not found in AD169. HCMV microarrays were spotted onto poly-lysine-coated glass microscope slides by using a Genemachines Omnigrid 100 arrayer (Genomic Solutions, Ann Arbor, Mich.) and SMP3 pins (Telechem, Sunnyvale, Calif.) following standard procedures (http://cmgm.stanford.edu/pbrown/protocols/1_slides.html). Each oligonucleotide representing a single ORF was printed in quadruplicate onto the slide at a concentration of 25 μM in 3× SSC (1× SSC is 0.15 M NaCl plus 0.015 M sodium citrate). After printing, the slides were postprocessed (http://cmgm.stanford.edu/pbrown/protocols/3_postprocess.html) and stored in a desiccator at room temperature. The HCMV microarray was also spotted with 102 human genes, 6 designed by Sigma-Genosys and 96 from the Human OligoLibrary release 1.0 evaluation plate (Compugen, Jamesburg, N.J.). The complete gene list for the HCMV microarray can be found at http://www.cag.icph.org/microarray.html.

cDNA labeling and hybridization. To analyze global viral gene expression at each time point, HFF cells were infected with AD169VRS-Δ and AD169VRS-R for 8, 12, 24, 48, and 72 h. Total RNA was isolated from the infected cells by using TRIzol reagent (Gibco BRL, Rockville, Md.). Total RNA (3 μg) was reverse transcribed into cDNA in the presence of either cyanine 3-dUTP (Cy3) or cyanine 5-dUTP (Cy5) (Perkin-Elmer, Wellesley, Mass.) as described elsewhere (44). Prior to hybridization, the slides were blocked with a solution of 3% bovine serum albumin and 0.1% sodium dodecyl sulfate (SDS) for 1 h at 42°C. After blocking, the slides were washed in 100% isopropanol, rinsed with water, and dried by centrifugation. The purified cDNA was applied to the arrays in 10 μl of hybridization solution (labeled cDNA, 0.5 μg of tRNA/μl, 0.5 μg of salmon sperm DNA/μl, 2.0× SSC, 25% formamide, and 0.1% SDS), covered by a flat 22- by 22-mm coverslip (Corning, Corning, N.Y.), and sealed in hybridization chambers (GeneMachines, Ann Arbor, Mich.) for 16 h at 58°C. After hybridization, the coverslips were removed from the slides by submerging into a solution of 2× SSC–0.1% SDS. The slides were washed rigorously in a solution of 1× SSC–0.05% SDS followed by a solution of 0.06× SSC and spun dry by centrifugation. The complete protocol for labeling and hybridization can be found at the website http://www.cag.icph.org/microarray.html.

Image acquisition and data analysis. The slides were scanned using an Axon 4000A scanner at 532 and 635 nm. Images were processed using GenePix 5.1 (Molecular Devices Corporation, Union, Calif.) and the HCMV array file (http://www.cag.icph.org/microarray.html). Resulting text files were exported to Microsoft Excel. The data were filtered initially by removing all spots that were flagged as "bad" or below the background noise. Spots whose sum of the median intensities was less than twice the highest average background of the chip were considered below background. A scaling factor was calculated by selecting nine human control genes that were relatively stable over the time course of infection and dividing the ratio of the average median intensity of Cy5 by the average median intensity of Cy3. The GenBank accession numbers and names for the control genes are the following: X04238 (7 SK), NM_002046 (GAPD), NM_012423 (ribosomal protein L13a), NM_001614 (actin, gamma 1), NM_004039 (annexin A2), NM_001961 (EEF2), M17733 (thymosin beta-4), NM_000981 (ribosomal protein L19), and NM_000994 (ribosomal protein L32). The data were normalized by multiplying the Cy3 channel by the scaling factor. The ratio of the average median intensity of Cy5 over the average median intensity of Cy3 was determined for each spot. The filtered, normalized data then were loaded into GeneSpring (Silicon Genetics, Redwood, Calif.). The data were clustered based on the average ratios of the quadruplicate spots, using the standard correlation method.

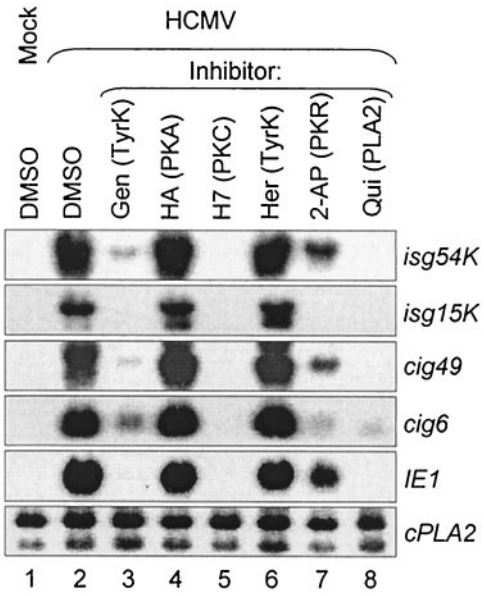

FIG. 1. The expression of ISGs and HCMV IE1 may require similar signal transduction pathways. HFF cells were mock infected or infected with HCMV in the absence of a kinase inhibitor (DMSO) or in the presence of kinase inhibitors, as indicated above the lanes. These inhibitors included the tyrosine kinase (TyrK) inhibitor genistein (Gen), the PKA inhibitor HA1004 (HA), the PKC inhibitor H7, the PKR inhibitor 2-AP, and the cPLA2 inhibitor quinacrine (Qui). The expression levels of *isg54K*, *isg15K*, *cig49*, *cig6*, and IE1 were measured by Northern blotting. cPLA2 was used as an internal control. Inhibitors that blocked *isg* expression also blocked HCMV IE1 expression.

RESULTS

The HCMV-initiated signal transduction pathway not only activates ISGs but may also stimulate HCMV IE expression. Both HCMV infection and IFN treatment can induce a large number of ISGs (50, 51). It is known that IFNs use the Jak-Stat signal transduction pathway to activate ISGs (10, 11); however, HCMV most likely activates ISGs in a different way than IFNs. HCMV disrupts the Jak-Stat pathway and likely uses a not-yet-identified pathway to effect ISG activation (28–30). To examine whether an HCMV-induced pathway has any effect on HCMV major IE expression, different kinase inhibitors were used to block ISG induction by HCMV. HFF cells were infected with HCMV for 8 h, and the expression of ISGs *isg54K*, *isg15K*, *cig49*, and *cig6* (51) was measured in the presence of different kinase inhibitors by Northern blot analysis. It was found that induction of ISGs by HCMV can be strongly inhibited or completely blocked by genistein (protein tyrosine kinase inhibitor), H7 (PKC inhibitor), quinacrine (phospholipase A2 inhibitor), and 2-AP (dsRNA-dependent kinase inhibitor), but this induction was not sensitive to HA1004 (PKA inhibitor) and herbimycin A (protein tyrosine kinase inhibitor) (Fig. 1). It is not clear why one tyrosine kinase inhibitor (genistein) can block ISG induction while the other (herbimycin) cannot. These results suggest that the activities of tyrosine kinase, PKC, dsRNA-dependent kinase, and phospholipase A2 are required for the HCMV-initiated signal transduction pathway.

More importantly, when HCMV IE1 expression in response to the above inhibitors was examined, we found that the inhib-

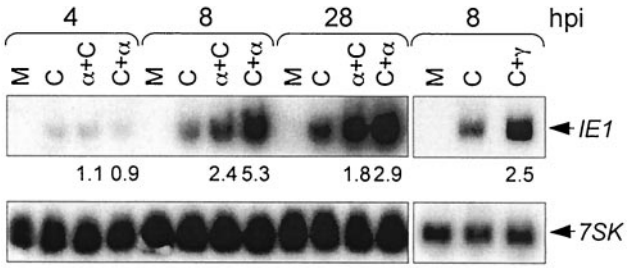

FIG. 2. IFNs stimulate HCMV major IE expression. HFF cells were either mock infected (M) or infected with HCMV (C) for different times as indicated above the lanes (hpi). The cells were treated with IFN-α or IFN-γ for 2 h before infection (α+C), 4 h after infection (C+α or C+γ), or left untreated (C). Northern blot assays were performed to measure HCMV IE1 expression. Fold activation of IE1 is indicated at the bottom of the upper panel. The cellular *7SK* gene was used as an internal control (lower panel).

itors that blocked ISG expression generally also blocked IE1 expression, and vice versa (Fig. 1), except for the dsRNA-dependent kinase inhibitor 2-AP, which appeared to have less of an effect on IE1 expression. This experiment implies that induction of ISGs and HCMV major IE genes may use a similar signal transduction pathway. Specifically, this HCMV-initiated signal transduction pathway may regulate viral major IE expression.

IFN-α and IFN-γ can stimulate HCMV IE1 expression. Results from the above experiment suggest that an HCMV-initiated signal pathway not only activates ISGs but also stimulates viral IE expression. If this hypothesis were correct, enhanced IE gene expression might be observed after HCMV-infected cells are treated with IFNs. Conversely, we also considered that this experiment might fail because HCMV infection may block IFN activity by disrupting the Jak-Stat signal transduction pathway, as has been reported elsewhere (28–30). To test the effect of IFNs on HCMV major IE gene expression, the IFN pathway was triggered by treating HFF cells with either IFN-α or IFN-γ at 2 h before or 4 h after HCMV infection. Indeed, when the cells were treated with IFNs, the HCMV IE1 mRNA level was increased up to fivefold (Fig. 2). A cellular *7SK* gene (37) was used as an internal control. The data suggest that under these experimental conditions, HCMV infection is not sufficient to block the IFN signaling that can stimulate HCMV major IE expression.

There are two VRS elements in the HCMV MIEP/E. Since IFN-α and IFN-γ are able to stimulate HCMV major IE expression, the HCMV MIEP/E should contain IFN response elements. Analysis of an approximately 1-kb fragment encompassing the AD169 MIEP/E (4) revealed no consensus sequence (AGTTTCNNTTTCNC) of ISRE. However, two identical 9-bp palindromic elements, TTACGGTAA, were identified which matched the consensus sequence of a GAS element (TTNCNNNAA). This element is named VRS1 for HCMV (virus) response site 1. The two VRS1 are located between −380 and −388 and between −502 and −510, respectively, and are separated by a 113-bp spacer. Our recent study has shown that VRS1 serves as an HCMV response site and is able to support transcriptional activation induced by UV-inactivated HCMV by specifically interacting with HCMV-activated proteins (47). These two VRS1 are not only present in the AD169 MIEP/E, but also the identical sequences and genome locations are found in other sequenced HCMV strains, including Towne, Toledo, Fix, TR, PH, and Merlin (12, 13, 36).

A VRS deletion mutation in the MIEP/E is manifested as a growth defect in HFF cells. Our hypothesis is that HCMV infection activates a signal transduction pathway that leads not only to induction of ISGs, but also activates the HCMV major IE gene through two VRS1 in the MIEP/E. To test this hypothesis directly, a 131-bp fragment (from −380 to −510) containing both VRS1 was deleted from the MIEP/E and the growth properties of this mutant virus were examined. A highly efficient BAC recombination system was used to generate this deletion virus (13). Briefly, a *kan/lacZ* cassette was amplified by PCR using two primers containing 40-bp sequences homologous to the flanking sequences of the two VRS1 in the MIEP/E. This PCR product was transformed into *E. coli* DY380 harboring $AD169_{BAC}$. The 131-bp VRS1 fragment was replaced by the *kan/lacZ* cassette by homologous recombination, resulting in blue, kanamycin-resistant colonies (Fig. 3A).

The correct deletion clone, named AD169VRS-Δ, was confirmed by PCR analysis (Fig. 3B). When the VRS1-specific primers were used (Fig. 3A, 1F and 1R), only $AD169_{BAC}$, but not AD169VRS-Δ, clones gave the expected 131-bp product (lanes 1 and 2). When the same analyses were performed using one primer inside the *kan/lacZ* cassette (2R and 3F) and one primer located in the junction region of the MIEP/E (Fig. 3A, 2F and 3R), the predicted left junction (634 bp) and right junction (1 kb) PCR fragments were amplified from the AD169VRS-Δ clones but not from $AD169_{BAC}$ (Fig. 3B, lanes 5 to 8). The viral UL4 ORF was used as a positive control, which was amplified from both wild-type and mutant templates (lanes 3 and 4). The AD169VRS-Δ clone was confirmed further by Southern blot analysis. The VRS element could be detected only in $AD169_{BAC}$, and not in the AD169VRS-Δ clone (Fig. 3C).

The AD169VRS-Δ DNA then was transfected into HFF cells, where the cytopathic effect evolved more slowly than in cells transfected with $AD169_{BAC}$ DNA, and high-titer AD169VRS-Δ virus production was unobtainable. This potential growth defect was confirmed by a multiple-step growth curve analysis. The peak titer of AD169VRS-Δ mutant virus was found to be 100- to 1,000-fold less than that of the $AD169_{BAC}$ virus (Fig. 3D). This experiment suggests that the 131-bp fragment containing the two VRS1 is important for HCMV replication.

Analyses of wild-type and mutant VRS activities in vitro. In addition to the two VRS1 sites, this 131-bp fragment also contains other transcription factor-binding sites, such as CREB. It is not clear whether the two VRS1 or other sequences within the 131-bp fragment of MIEP/E are important for HCMV IE gene expression. It may also be that the insertion of the *kan/lacZ* cassette in this region might have a negative effect on viral replication. To examine this, point mutations were introduced in each VRS1 site in the MIEP/E, and the replication properties of recombinant viruses containing these mutations were examined. To mutate the VRS and to facilitate further analysis of the mutants, the two VRS1 were engineered to include either XhoI or XbaI restriction enzyme sites. This mutagenesis strategy resulted in a single base-pair change (A to G) in the first GAS consensus sequence and two

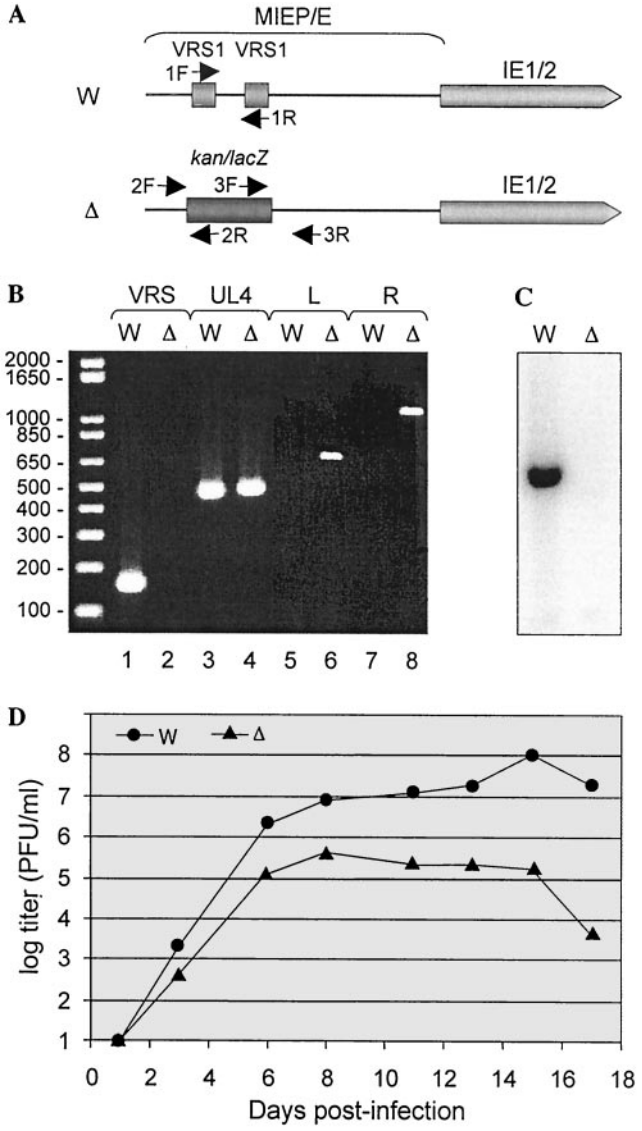

FIG. 3. Deletion analysis of two VRS1 elements in the HCMV major IE promoter. (A) The two VRS1 elements within a 131-bp fragment of wild-type $AD169_{BAC}$ (W) were replaced by a *kan/lacZ* cassette to generate a VRS1 deletion mutant, AD169VRS-Δ (Δ). The names, locations, and orientations of PCR primers for verifying the correct clones are indicated by arrows. (B) Using PCR, the deletion clone (Δ) was compared with the wild-type clone (W). The results showed that the VRS fragment was not present in the mutant clone (lane 2) but was present in the wild type (lane 1). The *kan/lacZ* cassette was inserted in the correct genomic position, as evidenced by the presence of the right (lane 8) and left (lane 6) junctions in the deletion clone but not in the wild-type clone (lanes 7 and 5). UL4 was used as a control (lanes 3 and 4). (C) The wild-type (W) and deletion (Δ) BAC DNAs were digested by EcoRI and SalI, and the deletion of VRS elements was confirmed further by Southern blotting using the VRS fragment as a probe. The VRS fragment is only present in the wild type (W) and not in the deletion (Δ) clones. (D) A multistep growth curve analysis was performed to compare the wild type (W; black circle) and VRS deletion mutant (Δ; black triangle) at an MOI of 0.1. The peak titer of mutant virus was 100- to 1,000-fold lower than that of the wild-type virus.

base-pair changes (C to T and A to G) in the second GAS consensus sequence (Fig. 4A).

Our previous studies demonstrated that double base-pair changes in the consensus sequence of GAS loci were sufficient to abolish the VRS transcriptional activity in response to both HCMV and IFNs and their DNA-binding activities (47). Here, the same assays were used to confirm the new VRS mutations. An episomal luciferase reporter plasmid driven by the *isg54* promoter was used for testing the transcriptional activity of the wild-type and mutant VRS elements. We have shown that UV-inactivated HCMV activates this reporter gene in a VRS-dependent manner (47). In this study, the ISRE in the *isg54K* promoter was replaced by the 131-bp fragment containing either the wild-type VRS1 or the mutated VRS1, resulting in two new reporter plasmids, pElu-VRS-W (wild type) and pElu-VRS-P (point mutation) (Fig. 4A). When these plasmids were transfected into HFF cells, high basal levels of luciferase activities were observed, and UV-HCMV could not further activate luciferase from either wild-type or mutant reporters (data not shown) (UV-HCMV was used in this assay to avoid viral IE1 and IE2 nonspecifically activating the reporter gene). This was likely due to the *cis*-acting elements located in this 131-bp fragment. This experiment was repeated using two similar reporter plasmids, pElu-GAS (wild type) and pElu-GAS^m (point mutation) (Fig. 4A), in which the 113-bp spacer sequence between two VRS elements was removed. In this case, UV-HCMV strongly activated luciferase from pElu-GAS, but not from pElu-GAS^m (Fig. 4B). This result demonstrated that the wild-type VRS1 is critical for responding to UV-HCMV infection. The same result was obtained when IFNs were used in this assay (data not shown).

When the wild-type and mutated 131-bp DNA fragments were amplified from pElu-VRS-W and pElu-VRS-P, radiolabeled, and incubated with the HCMV-infected nuclear extract in the EMSA, the wild-type, but not the mutated VRS fragment, specifically formed a complex with cellular proteins (Fig. 4C). This binding activity can be specifically competed by excess amounts of cold ISRE and GAS elements, but not by a nonrelated sequence (reference 47 and data not shown). Both luciferase assay and EMSA results indicated that the mutations in the two VRS1 element sequences disrupted VRS transcription and DNA-binding activity. The VRS-binding proteins remain to be determined.

Two VRS1 elements in HCMV MIEP/E are important for viral replication. To demonstrate the importance of the two VRS1 in the MIEP/E, the 131-bp mutated VRS fragment was cloned into pGEM-lox-zeo (Fig. 5A, diagram 1). As described above (Fig. 4A), the two VRS1 in this fragment were replaced by XhoI and XbaI restriction sites, resulting in three base-pair changes in the two GAS consensus sequences. The VRS/zeo^r cassette was amplified and transformed into *E. coli* DY380 carrying AD169VRS-Δ (Fig. 5A, diagrams 2 and 3). Homologous recombination led to an insertion of the mutated VRS1 fragment into the MIEP/E of AD169VRS-Δ and replacement of the *kan/lacZ* cassette, resulting in the AD169VRS-P-zeo clone (Fig. 5A, diagram 4). Using the same method, the VRS1 point mutations in AD169VRS-P-zeo were repaired by replacing the mutated fragment with a wild-type VRS1 fragment, resulting in a rescued clone, AD169VRS-R-zeo. Southern blot analysis of the AD169 BAC clones using the 131-bp VRS DNA

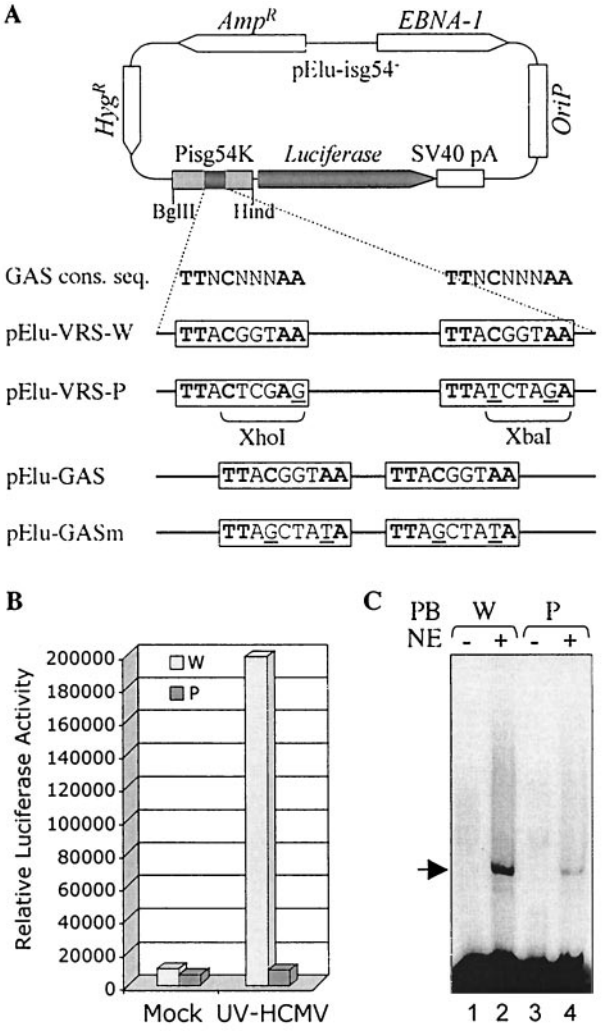

FIG. 4. Analyses of point mutations in the VRS elements. (A) The VRS1 wild-type and point mutation reporter plasmids, pElu-VRS-W and pElu-VRS-P, were constructed. A 131-bp MIEP/E fragment containing either wild-type or mutated VRS1 (as shown in boxes) was inserted into the *isg54K* promoter (Pisg54K) in pElu-NRS (47). In pElu-VRS-P, one VRS1 was converted into an XhoI site and the other was converted into an XbaI site as indicated, resulting in three point mutations in the GAS consensus sequences, as indicated by underlines. The GAS consensus sequence is also indicated. Two previously constructed VRS wild-type and mutant clones, pElu-GAS and pElu-GAS^m, also are illustrated. The intervening sequence between the two VRS1 elements in MIEP/E was removed in these two plasmids. (B) pElu-GAS and pElu-GAS^m were transfected into HFF cells. Ten days posttransfection, the cells were either mock infected (mock) or infected with UV-inactivated HCMV (UV-HCMV) at an MOI of 1 for 8 h, and luciferase assays were performed. The relative luciferase activities from the average of triplicate points are shown. (C) The DNA-binding activities of the wild-type and mutated VRS1-containing fragments were analyzed using EMSA. The 131-bp wild-type (W) and point mutation (P) fragments were amplified from pElu-VRS-W and pElu-VRS-P by PCR. These fragments were labeled as probes (PB) and incubated with or without HCMV-infected cell nuclear extracts (NE). A specific interaction was observed when the wild-type (lane 2), but not the mutant (lane 4), probe was used in the reaction.

fragment as a probe indicated that the VRS DNA fragments were present in the AD169$_{BAC}$, AD169VRS-P, and AD169VRS-R clones, but not in the AD169VRS-Δ clone (Fig. 5B, blot 1). The VRS1 point mutations were confirmed by PCR and restriction enzyme digestion. A 1.2-kb MIEP/E fragment was amplified from AD169VRS-P and digested with XhoI or XbaI. As expected, XhoI cut the mutated fragment into the 700- and 500-bp DNA fragments, and XbaI cut it into 620- and 580-bp DNA fragments (Fig. 5B, blot 2). As a control, the corresponding DNA fragment amplified from the AD169$_{BAC}$ and AD169VRS-R clones was not susceptible to digestion by XhoI or XbaI (data not shown).

To generate the VRS mutant and rescue viruses, AD169VRS-P-zeo and AD169VRS-R-zeo BAC DNAs were transfected into HFF cells. A Cre recombinase-expressing plasmid (49) was cotransfected with the viral DNAs so that the BAC vector and zeo^r cassette would be removed from the viral genome to produce AD169VRS-P and AD169VRS-R viruses (Fig. 5A, diagrams 5 and 6). Both resulting viruses were verified by PCR analyses. PCR showed that zeo^r selection markers were indeed removed from AD169VRS-P and AD169VRS-R genomes by Cre expression, and the marker was present in the original BAC clone (Fig. 5B, blot 3). It also showed that the VRS fragment was present in both AD169VRS-P and AD169VRS-R viruses, but not in the AD169VRS-Δ virus. HCMV gB was used as a positive control in this assay and was present in all tested viruses (Fig. 5B, blot 3). AD169VRS-P and AD169VRS-R viruses were confirmed by XhoI and XbaI digestions, as shown in Fig. 5B (blot 2). The 1.2-kb PCR fragments amplified from AD169VRS-P, but not from AD169VRS-R, were digested with XhoI and XbaI. This indicated that the two VRS1 were mutated as originally designed and that the rescue virus did not contain these mutations. Growth curve analysis confirmed that the rescue virus grows as well as the wild-type virus (data not shown).

The growth properties of AD169VRS-P and AD169VRS-R viruses at high and low MOIs were analyzed in growth curve analyses. Both viruses grew almost identically at an MOI equal to 1 (Fig. 5C, left panel), but AD169VRS-P grew significantly more slowly than AD169VRS-R at an MOI equal to 0.1 (right panel). The rescue virus reached a peak titer at about 10 days of infection, but the VRS1 mutant virus required about 16 days. In addition, the titer of the VRS mutant virus also was greater than 50-fold lower than that of the rescue virus. This result clearly demonstrated that the two VRS1 in the MIEP/E are crucial for efficient HCMV replication.

Two VRS1 elements are involved in regulation of HCMV major IE expression. Since mutations of the two VRS1 in the MIEP/E caused a slow growth phenotype of HCMV at a low MOI, this defect may be due to mutations that affect viral major IE expression. The expression of HCMV IE1 and IE2 was compared between mutant and rescue viruses. One criterion for this analysis was to ensure that equal amounts of the two viruses were used for inoculation. We noticed that the titer of the mutant virus was not necessarily accurate, because the growth defect at the low MOI underestimates the true number. To confirm AD169VRS-P and AD169VRS-R virus titers, HFF cells were infected with both viruses at an MOI equal to 1 for 2 h, and the tegument protein pp65 was measured by Western blotting (Fig. 6A). Equal amounts of pp65 were present in both

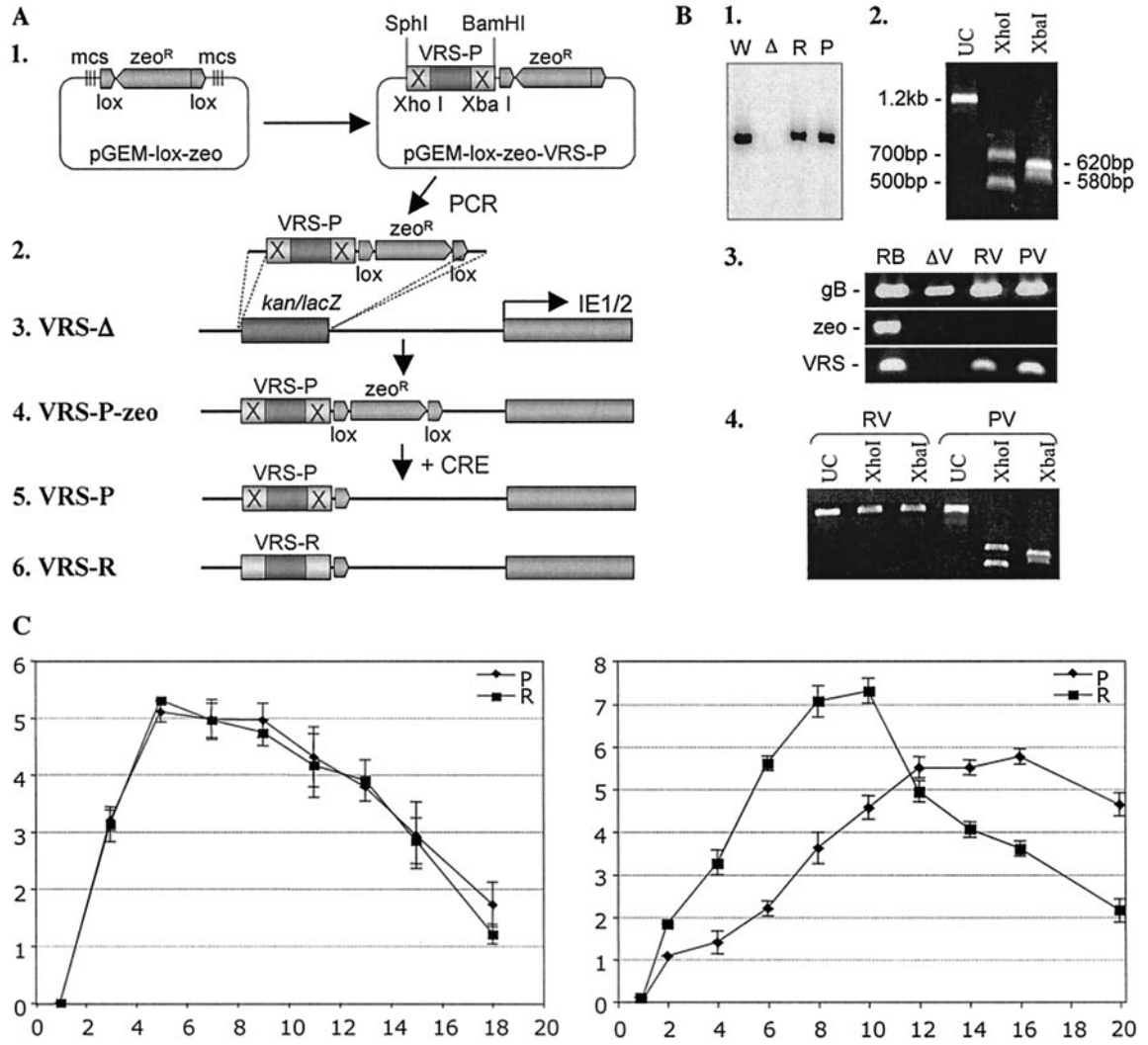

FIG. 5. Generation of the VRS1 point mutation and rescue viruses. (A, diagram 1) pGEM-lox-zeo was constructed by inserting a loxP/zeo^r cassette into pGEM-T. The 131-bp MIEP/E fragment containing the VRS1 mutations then was cloned between the SphI and BamHI sites of pGEM-lox-zeo to create pGEM-lox-zeo-VRS-P. The two VRS1 sites were converted into XhoI and XbaI, as shown in Fig. 4A. (Diagram 2) The VRS-P/zeo fragment was amplified by PCR. (Diagram 3) This PCR fragment was electroporated into DY380 carrying the AD169VRS-Δ BAC clone (VRS-Δ). (Diagram 4) The *kan/lacZ* fragment was replaced by the VRS-P/zeo to produce an HCMV clone containing mutated VRS1 elements with zeo^r (VRS-P-zeo). (Diagram 5) The VRS-P-zeo DNA was cotransfected with a CRE-expressing plasmid into HFF cells to generate the VRS1 point mutant (VRS-P), in which zeo^r was removed from the genome and one loxP site was left in the recombinant virus genome. (Diagram 6) A rescue virus (VRS-R) was generated using the same method, with the wild-type VRS1 replacing the mutated VRS1 in the MIEP/E. (B, blot 1) The VRS1 point mutation and rescue clones were confirmed by Southern blotting. The AD169VRS$_{BAC}$ (W), AD169VRS-Δ (Δ), AD169VRS-R (R), and AD169VRS-P (P) BAC DNA samples were digested with EcoRI and SalI, and Southern blot analysis was performed using a 131-bp probe containing the VRS sites. (Blot 2) The AD169VRS-P clone was confirmed by PCR. The 1.2-kb PCR product was either uncut (UC), cut by XhoI into 700 and 500 bp, or cut by XbaI into 620 and 580 bp. (Blot 3) The BAC DNAs were transfected into HFF cells to produce viruses. The correct recombinant viruses were verified by PCR. Glycoprotein B (gB), zeocin^r (zeo), and VRS-containing fragments were amplified from AD169VRS-Δ (ΔV), AD169VRS-P (PV), and AD169VRS-R (RV) viruses and AD169VRS-R BAC DNA (RB). (Blot 4) The 1.2-kb VRS fragment amplified by PCR from AD169VRS-R (RV) and AD169VRS-P (PV) viruses were either uncut (UC) or cut by XhoI or XbaI as indicated. (C) Growth curve analyses at an MOI of 1 (left panel) and an MOI of 0.1 (right panel) of AD169VRS-P (P) and AD169VRS-R (R) viruses. Each point was obtained from an average of triplicates.

samples of virus-infected cells, indicating that approximately equivalent amounts of virions were used for infection. Parenthetically, 30 and 10 μl of cell lysates were used to demonstrate the reaction was in the linear range. Actin was used as an internal control in this assay.

HCMV IE1 expression in the VRS1 mutant and rescue virus-infected cells was compared by Northern blotting. HFF cells were infected with either AD169VRS-P or AD169VRS-R at MOIs of 1 and 0.1 for different lengths of time. The results from Northern blot analysis showed that IE1 RNA levels were identical between both virus-infected cells at an MOI equal to 1, but they were dramatically reduced in the VRS1 mutant-infected cells at an MOI equal to 0.1 (Fig. 6B, row 1). Again, the *7SK* was used as an internal control (Fig. 6B, row 2).

IE1 and IE2 proteins were measured in a parallel experiment, and the same results were obtained. IE1 and IE2 protein

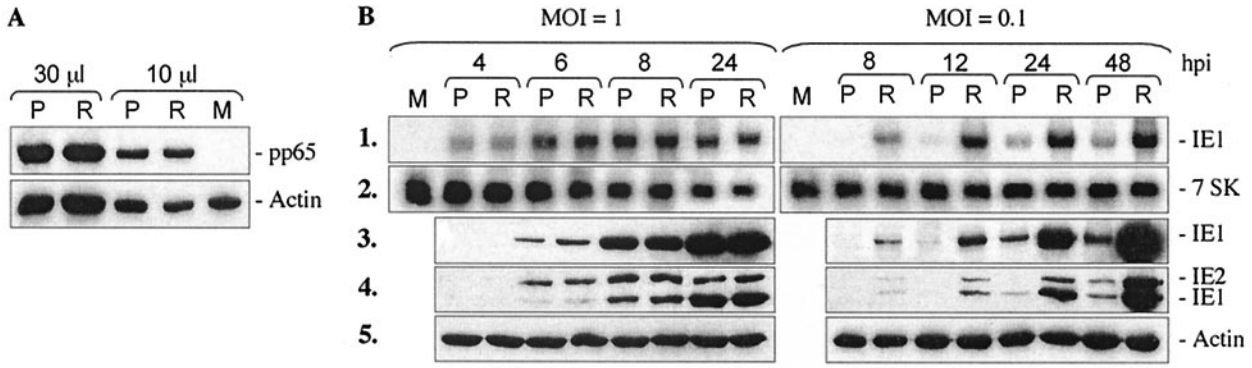

FIG. 6. The expression of IE1 and IE2 is reduced in AD169VRS-P infection. (A) HFF cells were mock infected (M) or infected with AD169VRS-P (P) or AD169VRS-R (R) virus at an MOI of 1 for 2 h. The infected cell lysates (30 and 10 μl) were analyzed by Western blotting using a monoclonal antibody against HCMV tegument protein pp65. Actin was used as an internal control. (B) Expression of HCMV IE1 and IE2 in the VRS1 mutant and rescue viruses was measured by Northern blotting and Western blotting. HFF cells were either mock infected (M) or infected with AD169VRS-P (P) or AD169VRS-R (R) virus at an MOI of 1 or 0.1. Total RNA and protein were prepared at the indicated hpi. The IE1 RNA level was measured by Northern blotting (row 1). A cellular 7 SK RNA was used as an internal control (row 2). The IE1 and IE2 protein levels were detected by Western blotting using anti-IE1 antibody, 1B12 (row 3), or anti-IE1/2 antibody mAB810 (row 4). Actin was used as an internal control (row 5).

levels were similar in both samples of virus-infected cells at a high MOI, but their levels were much lower for the VRS1 mutant virus at a low MOI (Fig. 6B, rows 3 and 4). Actin was used as an internal control (Fig. 6B, row 5). The results demonstrated that the mutation of two VRS1 in the MIEP/E caused a reduction in expression of IE1 and IE2.

IFNs no longer stimulate IE1 expression by the VRS1 mutant virus. We showed previously that IFN-α and IFN-γ could stimulate IE1 expression (Fig. 2), presumably by signaling through the two VRS1 in the MIEP/E. Whether IFNs could stimulate the IE expression in the VRS1 mutant virus was tested. HFF cells were infected with AD169VRS-P or AD169VRS-R virus. The infected cells were either untreated or treated with IFN-α or IFN-γ at 2 h postinfection (hpi). For the purposes of convenience, the IE protein, rather than RNA, was measured. Both IFN-α and IFN-γ could enhance IE1 levels of AD169VRS-R, but not AD169VRS-P (Fig. 7). This limited increase in IE1 levels in the rescued virus by IFN treatment might be due to a disruption of the Jak-Stat pathway by HCMV infection (28–30). This result indicates that the two VRS1 in the mutant virus are inactivated, which is also consistent with the results from the above in vitro functional analyses of the VRS1 mutation (Fig. 4).

The majority of genes in the VRS1 mutant virus were expressed at lower levels. Since the VRS1 mutation in the MIEP/E reduces IE1 and IE2 expression, we expected that the expression of other viral genes would be lower as well. To compare the global viral expression in the VRS1 mutant and rescue viruses, an HCMV microarray was used. HFF cells were infected with either AD169VRS-P or AD169VRS-R at an MOI of 0.1 for 8, 12, 24, 48, and 72 h. Total RNA was isolated from the infected cells, and cDNAs were prepared. The cDNAs from AD169VRS-P-infected cells were labeled with Cy3 and the cDNAs from AD169VRS-R-infected cells were labeled with Cy5, or vice versa. The two cDNA samples were mixed and hybridized on an HCMV microarray. After normalizing to nine human genes, the average intensities from four replicate spots of each ORF for each virus sample were obtained. Among 194 unique ORFs analyzed, 12 ORFs had signals that were close to background and were not considered further. The remaining 183 ORFs were clearly expressed, and the expression ratio for each of these ORFs from AD169VRS-R versus AD169VRS-P was obtained from averaging the data from three independent experiments (Fig. 8; see also Table S1 of the supplemental material).

In the cluster analysis, the ratio of each ORF in AD169VRS-R versus AD169VRS-P is indicated by the color intensity. The ORFs expressed at higher levels in AD169VRS-R than AD169VRS-P are indicated (Fig. 8A). Similar expression patterns were clustered together. As shown in Fig. 8A, the expression patterns could be clustered into four major groups. The first group includes 41 ORFs (22%) that were generally more highly expressed in AD169VRS-R than AD169VRS-P throughout the infectious cycle, especially at 12 and 48 hpi. As expected, IE1 and IE2 were within this group. US3 is also in this group (see Discussion). The result showing an effect on US3 expression was consistent with a previous finding that a distal enhancer deletion of MIEP/E caused an underproduction of US3 RNA (25). There were 37 ORFs (20%) in the second group. The patterns in this cluster were similar to those in

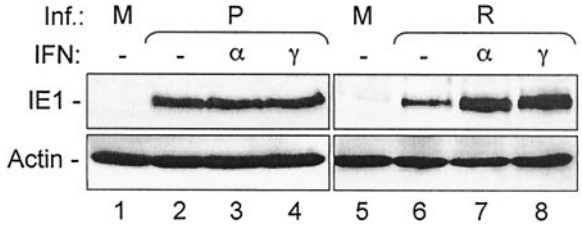

FIG. 7. IFNs failed to stimulate IE1 expression in the VRS1 mutant virus. HFF cells were either mock infected (M) or infected with the VRS1 mutant, AD169VRS-P (P), or the rescue virus, AD169VRS-R (R). The infected cells were then either untreated (lanes 2 and 6) or treated with IFN-α (lanes 3 and 7) or IFN-γ (lanes 4 and 8) at 2 hpi. HCMV IE1 protein was measured at 8 hpi by Western blotting using an anti-IE1 antibody, 1B12. Actin was used as an internal control.

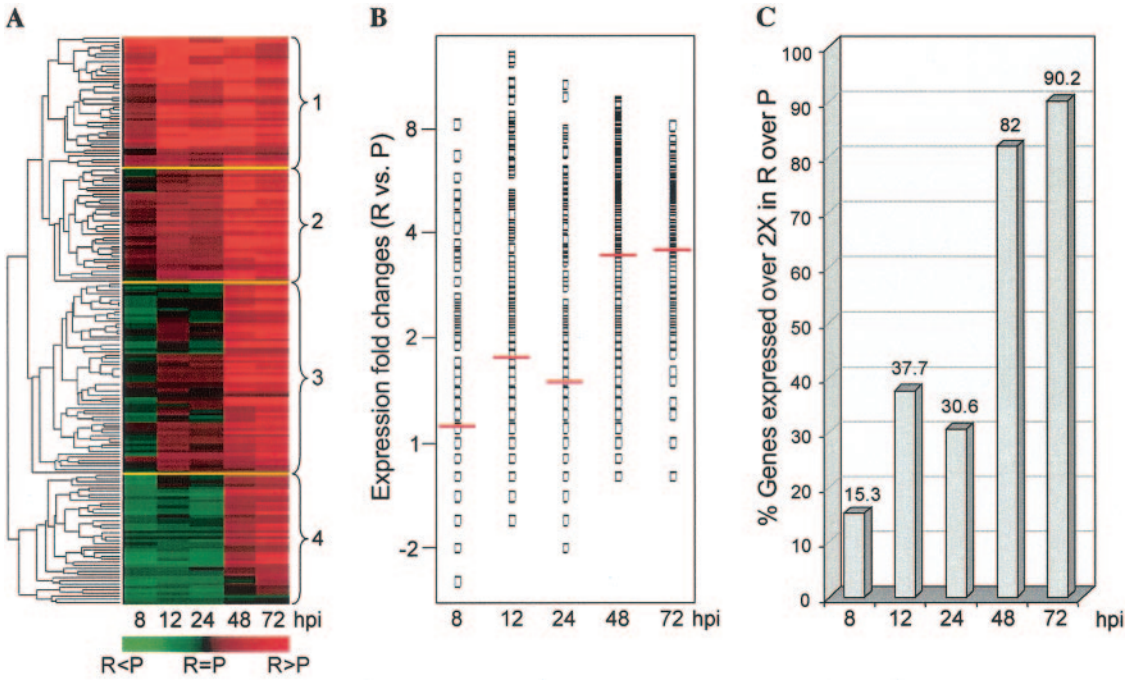

FIG. 8. Comparison of HCMV gene expression in AD169VRS-P and AD169VRS-R viruses in an HCMV microarray. HFF cells were infected with either the VRS1 point mutant virus (P) or the rescue virus (R) at an MOI of 0.1 for 8, 12, 24, 48, or 72 h. Total RNAs were isolated from the infected cells. The cDNA from AD169VRS-P-infected cells was labeled with Cy3, and the cDNA from AD169VRS-R-infected cells was labeled with Cy5. Equal amounts of cDNAs were mixed and hybridized to the HCMV microarrays. The expression of each ORF from both viruses was compared. (A) Cluster analysis. Four major clusters are divided by the yellow lines. The ORFs expressed higher in R than in P are indicated in red, the ORFs expressed lower in R than in P are indicated in green, and the ORFs expressed equally in R and P are indicated in black. (B) Expression fold changes (R over P) of 183 ORFs. Fold changes are represented by open squares and are in logarithmic scale. The geometric averages of fold changes at each time postinfection are indicated by the red bars. (C) Percentages of ORFs expressed above twofold in R versus P are indicated.

the first group, but the ratios between AD169VRS-R and AD169VRS-P were lower until 48 and 72 hpi. The third group contained 63 ORFs (35%). The majority of ORFs in this group did not show significant changes between the two viruses until 48 hpi. The last group had 42 ORFs (23%) that were expressed at higher levels in AD169VRS-P than AD169VRS-R in the first 24 hpi, and this pattern was reversed after 48 hpi. The UL9 gene is a good example in this group (see Discussion). The detailed cluster information can be found in Fig. S1 of the supplemental material.

The fold changes (AD169VRS-R over AD169VRS-P) of all 183 ORFs at each time point were plotted. As shown in Fig. 8B, except for a small number of ORFs that were shown to have markedly high fold changes, most ORFs were expressed at moderately higher levels for the first 24 hpi; the geometric averages of fold changes at 8, 12, and 24 hpi were 1.1, 1.7 and 1.5, respectively. However, the majority of ORFs were expressed significantly higher in AD169VRS-R than in AD169VRS-P after 48 hpi, and the geometric averages of fold changes at 48 and 72 hpi were increased to 3.5 and 3.6, respectively.

The numbers of ORFs expressed at higher levels in AD169VRS-R than AD169VRS-P were also calculated. At 8 hpi, only 15.3% of ORFs were expressed in AD169VRS-R at over twofold that of AD169VRS-P, and this number increased to 37.7, 30.6, 82, and 90.2% at 12, 24, 48, and 72 hpi (Fig. 8C).

Microarray analysis allowed us to begin to elucidate the consequence of the VRS1 mutations in the MIEP/E. At a low MOI, the VRS1 mutations caused an overall reduction of viral expression, especially at the late stages of infection.

DISCUSSION

In this study, we report a relationship between HCMV-mediated induction of ISGs and expression from the MIEP/E. HCMV infection triggers a signal transduction pathway that causes the activation of a large number of ISGs in HFF cells (50, 51). Herein, we extend this observation with data that indicate that HCMV major IE expression also seems to be regulated by this pathway, since the kinase inhibitors that block HCMV-induced ISG activation also block major IE expression, or vice versa. Since under certain conditions IFN-α and IFN-γ can stimulate HCMV major IE expression, the HCMV MIEP/E was examined. Two identical 9-bp palindromic elements, VRS1, between bp −380 and −510, were identified which matched the GAS consensus sequence. To demonstrate the importance of these two VRS1 elements, deletion and point mutation recombinant viruses were generated. Growth curve analyses showed that the VRS1 mutant viruses grew normally at a high MOI but grew poorly at a low MOI. This growth defect could be rescued completely when the wild-type VRS1 fragment was reinserted into the MIEP/E. The growth defect of the VRS1 mutant was due to impairment of viral

major IE expression, which led to a global reduction of viral gene expression.

Previous studies have shown that deletion of the distal enhancer region of the MIEP/E (bp −300 to −582 or −640) greatly affects HCMV replication in HFF cells at a low MOI (25). These results imply that the important regulatory elements for major IE expression are located within the deleted 280-bp region. However, this is a large deletion which contains Ets, SRE, CREB/ATF, NF-κB, and SP1 transactivator-binding sites (33), and it was unclear which element(s) was critical for replication. In this study, the control region was localized to a 131-bp region (bp −380 to −510) by using the AD169VRS-Δ mutant.

Within this region of the MIEP/E, there are two identical palindromic sequences, VRS1 (TTACGGTAA), which were matched to the consensus sequence of the GAS element (TT NCNNNAA). These sequences were conserved in all HCMV strains examined. Although three base-pair substitutions in the consensus GAS sequences are sufficient to produce the slow growth phenotype at a low MOI, it is not clear whether the VRS1 is functionally identical to the GAS element and whether the palindromic sequence or the GAS consensus sequence is more critical for responding to the HCMV-initiated signal pathway and regulating major IE expression. This question will be answered when more VRS1 base-pair substitution mutants have been generated and tested. Interestingly, in addition to these two VRS1 in the MIEP/E, only one identical VRS1 element is present in all the sequenced HCMV genomes. It is located in the promoter region of the UL36-37 immediate-early locus. The function of this VRS element in this region remains to be determined. On the other hand, hundreds of consensus GAS sequences were found in the HCMV Merlin genome, raising a question of how many of them are specific and functional.

The growth defect of the VRS1 mutant is likely caused directly by disruption of VRS1 function in the MIEP/E, not by interference with the expression of neighboring non IE ORFs or by a 34-bp loxP insertion (Fig. 5A, diagram 5). The only ORF near the mutated region is UL124. It is unlikely that the growth defect of the VRS1 mutant is caused by the altered UL124 function, because UL124 is located between bp +475 and +934, which is distant from the VRS1 mutations. The remaining loxP site in the MIEP/E does not appear to have any effect on viral growth because the rescued virus, AD169VRS-P, which contains the loxP site at the same position (Fig. 5A, diagram 6), grows as well as the true wild-type virus (data not shown).

While it is clear from this study that the two VRS1 elements in the MIEP/E are important for major IE expression and viral growth in HFF cells at a low MOI, we propose that the HCMV-initiated signal transduction pathway, which leads to the activation of ISGs, directly regulates major IE expression through the VRS1 sites. Previously, we showed that when these two VRS1 were inserted upstream of a luciferase reporter gene, the reporter was strongly activated upon infection of cells harboring this plasmid with UV-inactivated HCMV. In contrast, the reporter was not activated under the same conditions in cells harboring a similar plasmid that contains point mutations in the VRS sites (Fig. 4B) (47). Furthermore, cellular proteins can form specific complexes with the wild-type but not the mutant VRS, and this interaction is strongly induced by HCMV infection (Fig. 4B) (47). Taken together, the evidence suggests that HCMV uses a signal transduction pathway to regulate major IE expression through the VRS sites in the MIEP/E. The molecular mechanism of this regulation will become clear when this HCMV-initiated signal transduction pathway and HCMV-activated VRS-binding proteins have been characterized more thoroughly.

The defective growth of the VRS1 mutant virus at a low MOI suggests that the VRS1 elements in MIEP/E are physiologically important, because HCMV infection or reactivation in vivo is probably most analogous to a low-MOI infection. High MOI may be achieved only in vitro, and many defective phenotypes cannot be observed at high MOI, including the IE1 mutants, the MIE enhancer deletion mutants, and the UL82 (pp71) mutant (6, 15, 16, 18, 25, 34). The mechanism of how a high MOI can bypass the VRS mutation defect has not been elucidated. However, it is not likely due to increased viral genomic template because an MOI of 1, which is not more than one infectious copy per cell, is sufficient to overcome the defect. At an MOI of 1, however, infectious particles, plus many more noninfectious particles, may cause activation of the signal transduction pathways and/or deliver a sufficient dose of virion tegument proteins to stimulate IE1 and IE2 expression and thereby compensate for the VRS1 mutations. The pp71 tegument protein is such a candidate. It dramatically stimulates the infectivity of viral DNA and major IE expression (1).

Generation of the VRS1 mutant virus and its rescue virus allowed us to explore IE1 and IE2 functions on viral gene expression and replication in a direct manner. Transient-transfection assays showed that the IE1 and IE2 proteins are potent transcription factors that cooperatively activate transcription from many promoters, including HCMV early promoters (9, 21, 23). However, these transient-transfection assays do not reflect the actual infection situation. Construction of the IE2 deletion temperature-sensitive clones proved that IE2 is essential for viral replication and is absolutely necessary for HCMV early gene expression (17, 24). Nevertheless, it is impossible to understand completely IE1 and IE2 function during infection with these mutants. In the present study, the VRS1 mutations in the MIEP/E greatly reduced IE1 and IE2 expression and provided an excellent model with which to study the consequences of IE1 and IE2 deficiency.

HCMV microarrays were used to measure viral gene expression at an MOI equal to 0.1 during the course of a single infectious cycle, within the first 72 hpi. The HCMV microarray analysis revealed some interesting phenomena. First, considering reduced IE1/2 expression of the VRS1 mutant virus, we assumed that there would be an overall reduction in expression of HCMV genes during infection with the VRS1 mutant virus. This is the case at 48 and 72 hpi, where approximately 82 and 90% of genes, respectively, are expressed at significantly lower levels in the mutant virus than the rescue virus. This is in contrast to gene expression during the first 24 hpi. At 8 to 24 hpi, 14 to 37% of genes were expressed at significantly lower levels in the mutant virus than in the rescue virus. In addition to IE1 and IE2, the ORFs in these latter groups should contain the genes that are strongly dependent on IE1/2 function in the early course of infection. US3 is a good example from this group. US3 is an IE gene and has an immune evasion functions

(20, 31, 32). Since it is an IE gene, it was expected that IE1/2 might not regulate its expression and its level might not be changed in the VRS1 mutant. However, the microarray data showed that US3 RNA was greatly diminished in the VRS1 mutant virus during the course of infection. The similar phenotype also was observed previously in a MIEP distal enhancer deletion mutant (25). This result suggests that the IE1 and IE2 proteins directly regulate US3 expression. This is supported by a study showing that IE1 and IE2 are able to activate the US3 promoter in transient-transfection assays (2, 3).

Secondly, and somewhat unexpectedly, several genes were expressed at higher levels within the first 24 hpi in VRS1 mutant virus-infected cells than in rescue virus-infected cells. This group of genes may be less dependent on IE1 and IE2, and their expression may be repressed by IE1 and IE2 in the early phase of infection. An interesting ORF in this group is UL9. In the first 24 h of infection, the UL9 RNA level is about 2- to 2.5-fold higher in the VRS1 mutant virus-infected cells than in the rescue virus-infected cells. This suggests that IE1 and IE2 proteins negatively regulate UL9 expression. Furthermore, a high level of UL9 may have a negative effect on viral growth. Although the function of UL9 is unknown, interestingly, a UL9 deletion mutant grows over 10 times better than the wild-type virus (13).

This study demonstrates that an HCMV-initiated signal transduction pathway stimulates major IE gene expression through two VRS1 elements in the MIEP/E. This mechanism also could be used by cytokines, especially during the course of HCMV reactivation from latency. The effects of tumor necrosis factor alpha and IFN-γ on HCMV replication have been demonstrated in macrophage cultures, which provide a valuable in vitro model system for the study of HCMV replication, latency, and reactivation (41). While both cytokines have antiviral activity, the addition of IFN-γ and tumor necrosis factor alpha to permissive monocyte-derived macrophages (MDM) did not inhibit viral production (42). Similar experiments determined the cellular and cytokine factors necessary for HCMV growth in MDM. It was found that $CD4^+$ and $CD8^+$ T cells, as well as interleukin-2 and IFN-γ, are required. IFN-γ not only is a critical factor in MDM permissiveness for HCMV production but also is a critical factor in the reactivation of latent HCMV in MDM (41).

The results presented in this study demonstrate that the two VRS1 elements in the HCMV MIEP/E are critical for HCMV replication at low MOI and suggest that the HCMV-initiated signal transduction pathway not only induces ISGs but also stimulates its own major IE expression.

ACKNOWLEDGMENTS

We thank T. Shenk for providing $AD169_{BAC}$ and pGEM/T-Pac-1-Kan/LacZ, L. Enquist for providing pGS403, and N. Copeland and C. Stranthdee for providing the DY380 strain of *E. coli*. We are grateful to C. Patterson and T. R. Jones for critically reading the manuscript.

This work was supported by NIH grant AI050709-01 (H.Z.).

REFERENCES

1. **Baldick, C. J., Jr., A. Marchini, C. E. Patterson, and T. Shenk.** 1997. Human cytomegalovirus tegument protein pp71 (ppUL82) enhances the infectivity of viral DNA and accelerates the infectious cycle. J. Virol. **71:**4400–4408.
2. **Biegalke, B. J.** 1999. Human cytomegalovirus US3 gene expression is regulated by a complex network of positive and negative regulators. Virology **261:** 155–164.
3. **Biegalke, B. J.** 1997. IE2 protein is insufficient for transcriptional repression of the human cytomegalovirus US3 promoter. J. Virol. **71:**8056–8060.
4. **Boshart, M., F. Weber, G. Jahn, K. Dorsch-Hasler, B. Fleckenstein, and W. Schaffner.** 1985. A very strong enhancer is located upstream of an immediate early gene of human cytomegalovirus. Cell **41:**521–530.
5. **Boyle, K. A., R. L. Pietropaolo, and T. Compton.** 1999. Engagement of the cellular receptor for glycoprotein B of human cytomegalovirus activates the interferon-responsive pathway. Mol. Cell. Biol. **19:**3607–3613.
6. **Bresnahan, W. A., and T. E. Shenk.** 2000. UL82 virion protein activates expression of immediate early viral genes in human cytomegalovirus-infected cells. Proc. Natl. Acad. Sci. USA **97:**14506–14511.
7. **Britt, W. J., and C. A. Alford.** 1996. Cytomegalovirus, p. 2493–2523. *In* B. N. Fields, D. M. Knipe, and P. M. Howley (ed.), Fields virology, 3rd ed. Lippincott-Raven Publishers, Philadelphia, Pa.
8. **Castillo, J. P., and T. F. Kowalik.** 2004. HCMV infection: modulating the cell cycle and cell death. Int. Rev. Immunol. **23:**113–139.
9. **Chang, C. P., D. H. Vesole, J. Nelson, M. B. Oldstone, and M. F. Stinski.** 1989. Identification and expression of a human cytomegalovirus early glycoprotein. J. Virol. **63:**3330–3337.
10. **Darnell, J. E., Jr.** 1998. Studies of IFN-induced transcriptional activation uncover the Jak-Stat pathway. J. Interferon Cytokine Res. **18:**549–554.
11. **Darnell, J. E., Jr., I. M. Kerr, and G. R. Stark.** 1994. Jak-STAT pathways and transcriptional activation in response to IFNs and other extracellular signaling proteins. Science **264:**1415–1421.
12. **Dolan, A., C. Cunningham, R. D. Hector, A. F. Hassan-Walker, L. Lee, C. Addison, D. J. Dargan, D. J. McGeoch, D. Gatherer, V. C. Emery, P. D. Griffiths, C. Sinzger, B. P. McSharry, G. W. Wilkinson, and A. J. Davison.** 2004. Genetic content of wild-type human cytomegalovirus. J. Gen. Virol. **85:** 1301–1312.
13. **Dunn, W., C. Chou, H. Li, R. Hai, D. Patterson, V. Stolc, H. Zhu, and F. Liu.** 2003. Functional profiling of a human cytomegalovirus genome. Proc. Natl. Acad. Sci. USA **100:**14223–14228.
14. **Fortunato, E. A., A. K. McElroy, I. Sanchez, and D. H. Spector.** 2000. Exploitation of cellular signaling and regulatory pathways by human cytomegalovirus. Trends Microbiol. **8:**111–119.
15. **Gawn, J. M., and R. F. Greaves.** 2002. Absence of IE1 p72 protein function during low-multiplicity infection by human cytomegalovirus results in a broad block to viral delayed-early gene expression. J. Virol. **76:**4441–4455.
16. **Greaves, R. F., and E. S. Mocarski.** 1998. Defective growth correlates with reduced accumulation of a viral DNA replication protein after low-multiplicity infection by a human cytomegalovirus ie1 mutant. J. Virol. **72:**366–379.
17. **Heider, J. A., W. A. Bresnahan, and T. E. Shenk.** 2002. Construction of a rationally designed human cytomegalovirus variant encoding a temperature-sensitive immediate-early 2 protein. Proc. Natl. Acad. Sci. USA **99:**3141–3146.
18. **Isomura, H., and M. F. Stinski.** 2003. The human cytomegalovirus major immediate-early enhancer determines the efficiency of immediate-early gene transcription and viral replication in permissive cells at low multiplicity of infection. J. Virol. **77:**3602–3614.
19. **Jones, T. R., L. K. Hanson, L. Sun, J. S. Slater, R. M. Stenberg, and A. E. Campbell.** 1995. Multiple independent loci within the human cytomegalovirus unique short region down-regulate expression of major histocompatibility complex class I heavy chains. J. Virol. **69:**4830–4841.
20. **Jones, T. R., E. J. Wiertz, L. Sun, K. N. Fish, J. A. Nelson, and H. L. Ploegh.** 1996. Human cytomegalovirus US3 impairs transport and maturation of major histocompatibility complex class I heavy chains. Proc. Natl. Acad. Sci. USA **93:**11327–11333.
21. **Klucher, K. M., M. Sommer, J. T. Kadonaga, and D. H. Spector.** 1993. In vivo and in vitro analysis of transcriptional activation mediated by the human cytomegalovirus major immediate-early proteins. Mol. Cell. Biol. **13:**1238–1250.
22. **Lopez-Botet, M., A. Angulo, and M. Guma.** 2004. Natural killer cell receptors for major histocompatibility complex class I and related molecules in cytomegalovirus infection. Tissue Antigens **63:**195–203.
23. **Malone, C. L., D. H. Vesole, and M. F. Stinski.** 1990. Transactivation of a human cytomegalovirus early promoter by gene products from the immediate-early gene IE2 and augmentation by IE1: mutational analysis of the viral proteins. J. Virol. **64:**1498–1506.
24. **Marchini, A., H. Liu, and H. Zhu.** 2001. Human cytomegalovirus with IE-2 (UL122) deleted fails to express early lytic genes. J. Virol. **75:**1870–1878.
25. **Meier, J. L., and J. A. Pruessner.** 2000. The human cytomegalovirus major immediate-early distal enhancer region is required for efficient viral replication and immediate-early gene expression. J. Virol. **74:**1602–1613.
26. **Meier, J. L., and M. F. Stinski.** 1996. Regulation of human cytomegalovirus immediate-early gene expression. Intervirology **39:**331–342.
27. **Michaelis, M., R. Kotchetkov, J. U. Vogel, H. W. Doerr, and J. Cinatl, Jr.** 2004. Cytomegalovirus infection blocks apoptosis in cancer cells. Cell Mol. Life Sci. **61:**1307–1316.
28. **Miller, D. M., C. M. Cebulla, and D. D. Sedmak.** 2002. Human cytomegalovirus inhibition of major histocompatibility complex transcription and interferon signal transduction. Curr. Top. Microbiol. Immunol. **269:**153–170.

29. **Miller, D. M., B. M. Rahill, J. M. Boss, M. D. Lairmore, J. E. Durbin, J. W. Waldman, and D. D. Sedmak.** 1998. Human cytomegalovirus inhibits major histocompatibility complex class II expression by disruption of the Jak/Stat pathway. J. Exp. Med. **187:**675–683.
30. **Miller, D. M., Y. Zhang, B. M. Rahill, W. J. Waldman, and D. D. Sedmak.** 1999. Human cytomegalovirus inhibits IFN-alpha-stimulated antiviral and immunoregulatory responses by blocking multiple levels of IFN-alpha signal transduction. J. Immunol. **162:**6107–6113.
31. **Misaghi, S., Z. Y. Sun, P. Stern, R. Gaudet, G. Wagner, and H. Ploegh.** 2004. Structural and functional analysis of human cytomegalovirus US3 protein. J. Virol. **78:**413–423.
32. **Mocarski, E.** 2001. Cytomegaloviruses and their replication, p. 2629–2673. *In* D. M. Knipe et al. (ed.), Fields virology, 4th ed., vol. 2. Lippincott Williams & Wilkins, Philadelphia, Pa.
33. **Mocarski, E. S.** 1996. Cytomegaloviruses and their replication, p. 2447–2492. *In* B. N. Fields, D. M. Knipe, and P. M. Howley (ed.), Fields virology, 3rd ed. Lippincott-Raven, Philadelphia, Pa.
34. **Mocarski, E. S., G. W. Kemble, J. M. Lyle, and R. F. Greaves.** 1996. A deletion mutant in the human cytomegalovirus gene encoding IE1 (491aa) is replication defective due to a failure in autoregulation. Proc. Natl. Acad. Sci. USA **93:**11321–11326.
35. **Murphy, E., I. Rigoutsos, T. Shibuya, and T. E. Shenk.** 2003. Reevaluation of human cytomegalovirus coding potential. Proc. Natl. Acad. Sci. USA **100:** 13585–13590.
36. **Murphy, E., D. Yu, J. Grimwood, J. Schmutz, M. Dickson, M. A. Jarvis, G. Hahn, J. A. Nelson, R. M. Myers, and T. E. Shenk.** 2003. Coding potential of laboratory and clinical strains of human cytomegalovirus. Proc. Natl. Acad. Sci. USA **100:**14976–14981.
37. **Murphy, S., F. Altruda, E. Ullu, M. Tripodi, L. Silengo, and M. Melli.** 1984. DNA sequences complementary to human 7 SK RNA show structural similarities to the short mobile elements of the mammalian genome. J. Mol. Biol. **177:**575–590.
38. **Netterwald, J. R., T. R. Jones, W. J. Britt, S. J. Yang, I. P. McCrone, and H. Zhu.** 2004. Postattachment events associated with viral entry are necessary for induction of interferon-stimulated genes by human cytomegalovirus. J. Virol. **78:**6688–6691.
39. **Sanchez, V., K. D. Greis, E. Sztul, and W. J. Britt.** 2000. Accumulation of virion tegument and envelope proteins in a stable cytoplasmic compartment during human cytomegalovirus replication: characterization of a potential site of virus assembly. J. Virol. **74:**975–986.
40. **Simmen, K. A., J. Singh, B. G. Luukkonen, M. Lopper, A. Bittner, N. E. Miller, M. R. Jackson, T. Compton, and K. Fruh.** 2001. Global modulation of cellular transcription by human cytomegalovirus is initiated by viral glycoprotein B. Proc. Natl. Acad. Sci. USA **98:**7140–7145.
41. **Soderberg-Naucler, C., K. N. Fish, and J. A. Nelson.** 1998. Growth of human cytomegalovirus in primary macrophages. Methods **16:**126–138.
42. **Soderberg-Naucler, C., K. N. Fish, and J. A. Nelson.** 1997. Interferon-gamma and tumor necrosis factor-alpha specifically induce formation of cytomegalovirus-permissive monocyte-derived macrophages that are refractory to the antiviral activity of these cytokines. J. Clin. Investig. **100:**3154–3163.
43. **Swaminathan, S., H. M. Ellis, L. S. Waters, D. Yu, E. C. Lee, D. L. Court, and S. K. Sharan.** 2001. Rapid engineering of bacterial artificial chromosomes using oligonucleotides. Genesis **29:**14–21.
44. **Voskuil, M. I., D. Schnappinger, K. C. Visconti, M. I. Harrell, G. M. Dolganov, D. R. Sherman, and G. K. Schoolnik.** 2003. Inhibition of respiration by nitric oxide induces a Mycobacterium tuberculosis dormancy program. J. Exp. Med. **198:**705–713.
45. **Wang, X., S. M. Huong, M. L. Chiu, N. Raab-Traub, and E. S. Huang.** 2003. Epidermal growth factor receptor is a cellular receptor for human cytomegalovirus. Nature **424:**456–461.
46. **White, E. A., C. L. Clark, V. Sanchez, and D. H. Spector.** 2004. Small internal deletions in the human cytomegalovirus IE2 gene result in nonviable recombinant viruses with differential defects in viral gene expression. J. Virol. **78:** 1817–1830.
47. **Yang, S., J. Netterwald, W. Wang, and H. Zhu.** 2005. Characterization of the elements and proteins responsible for interferon-stimulated gene induction by human cytomegalovirus. J. Virol. **79:**5027–5034.
48. **Yu, D., H. M. Ellis, E. C. Lee, N. A. Jenkins, N. G. Copeland, and D. L. Court.** 2000. An efficient recombination system for chromosome engineering in Escherichia coli. Proc. Natl. Acad. Sci. USA **97:**5978–5983.
49. **Yu, D., G. A. Smith, L. W. Enquist, and T. Shenk.** 2002. Construction of a self-excisable bacterial artificial chromosome containing the human cytomegalovirus genome and mutagenesis of the diploid TRL/IRL13 gene. J. Virol. **76:**2316–2328.
50. **Zhu, H., J. P. Cong, G. Mamtora, T. Gingeras, and T. Shenk.** 1998. Cellular gene expression altered by human cytomegalovirus: global monitoring with oligonucleotide arrays. Proc. Natl. Acad. Sci. USA **95:**14470–14475.
51. **Zhu, H., J. P. Cong, and T. Shenk.** 1997. Use of differential display analysis to assess the effect of human cytomegalovirus infection on the accumulation of cellular RNAs: induction of interferon-responsive RNAs. Proc. Natl. Acad. Sci. USA **94:**13985–13990.
52. **Zhu, H., Y. Shen, and T. Shenk.** 1995. Human cytomegalovirus IE1 and IE2 proteins block apoptosis. J. Virol. **69:**7960–7970.